Tokyo Climate Center, Japan Meteorological Agency

TCC News

Summer 2021

Table of Contents: TCC News No. 65

JMA's New Climatological Normals for 1991-2020

1. Introduction

Climatological normals are used as a base for comparison of current conditions, as well as to describe average climatic conditions. Under the Technical Regulations of the World Meteorological Organization (WMO-No. 49), climatological standard normals are averages of climatological data computed for the following consecutive periods of 30 years: 1 January, 1981, to 31 December, 2010; 1 January, 1991, to 31 December, 2020, and so forth. Countries should calculate climatological standard normals as soon as possible after the end of a standard normal period.

JMA has developed new climatological normals using climatological data for the period from 1991 to 2020, and started operationally using them on 19 May, 2021. The climatological normals specified below are used in a number of products available on the TCC website. Some of their details are summarized in the following sections.

- Climatological normals of surface observation stations in Japan as used in products available in the Climate in Japan section (Section 2)
- For global mean surface temperature, anomalies for individual surface observations are calculated in relation to the 1991 – 2020 average before being averaged over the globe (Section 3).
- Monthly climatological normals of surface observation stations around the world (temperature and precipitation) as used in products available in the World Climate section (Section 4)
- Climatological normals of oceanographic data based on Daily Sea Surface Analysis for Climate Monitoring and Predictions (COBE-SST) and the Ocean Data Assimilation System (MOVE/MRI.COM-G2) as used in products available in the El Niño Monitoring section (Section 5)
- Climatological normals of atmospheric circulation fields calculated using data of the Japanese 55-year Reanalysis (JRA-55) as used in products available in the Climate System Monitoring section (Section 6)

(WAKAMATSU Shunya, Tokyo Climate Center)

2. Climatological Normals of Surface Observation Stations in Japan

The new climate normals of seasonal mean temperatures tend to be 0.2 – 0.4°C higher than the old ones for most seasons and regions. Table 1-1 shows the differences between new and old climate normals for summer (June – August) and winter (December – February) mean temperatures in each region (Figure 1-1 left). Table 1-1 also shows frequencies for each tercile category in 1991 – 2020 based on the old climate normals (1981 – 2010 baseline). During this period, years with above-normal temperatures are often observed, reflecting a rise in the climatic temperature normal for summer in particular. By way of example, the above-normal occurrence ratio is 50 – 60% (16 to 18 events over the 30-year period) for summer and around 40% (11 to 13 events) for winter.

Table 1-2 shows the ratios of new to old climate normals for seasonal precipitation amounts in each region (Figure 1-1 right). The new values tend to be around 10% higher for most seasons and regions, with exceptions including summer on the Pacific side of eastern Japan, winter in Okinawa and Amami, and spring in western Japan (not shown).

Table 1-1 Differences between new and old climate normals for seasonal mean temperatures (left) and frequencies for each tercile category in 1991 – 2020 based on the old climate normals (right)

Region	Differences [1] (new – old climate normals)		Frequencies for each tercile category in 1991 – 2020 (based on old climate normals) [2]					
	Summer (Jun. – Aug.)	Winter (Dec. – Feb.)	Summer (Jun. – Aug.)			Winter (Dec. – Feb.)		
			–	0	+	–	0	+
Northern Japan	+0.4°C	+0.3°C	5	8	17	6	12	12
Eastern Japan	+0.4°C	+0.3°C	4	9	17	10	8	12
Western Japan	+0.2°C	+0.3°C	6	8	16	9	10	11
Okinawa and Amami	+0.3°C	+0.3°C	4	8	18	6	11	13

[1] Positive values indicate new normals higher than old ones.
[2] In cases with a limited difference between new and old climate normals, the frequencies of each tercile category would be 33% (i.e., 10 events over the 30-year period).

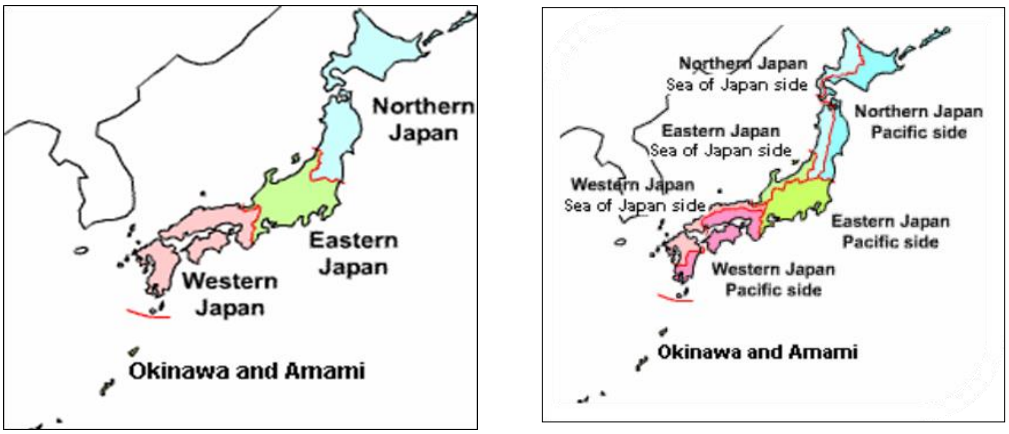

Figure 1-1 Regionalization for temperatures (left) and precipitation amounts (right)

Table 1-2 Ratios of new to old climate normals for seasonal precipitation amounts (left) and frequencies for each tercile category in 1991 – 2020 based on old climate normals (right)

Region	Ratios [1] (new – old climate normals)		Frequencies for each tercile category in 1991 – 2020 based on old climate normals [2]					
	Summer (Jun. – Aug.)	Winter (Dec. – Feb.)	Summer (Jun. – Aug.)			Winter (Dec. – Feb.)		
			–	0	+	–	0	+
Sea of Japan side of northern Japan	109%	104%	5	11	14	7	8	15
Pacific side of northern Japan	102%	107%	10	10	10	6	11	13
Sea of Japan side of eastern Japan	105%	103%	6	13	11	8	9	13
Pacific side of eastern Japan	98%	108%	10	12	8	7	12	11
Sea of Japan side of western Japan	104%	107%	8	10	12	7	10	13
Pacific side of western Japan	109%	111%	6	10	14	5	12	13
Okinawa and Amami	107%	99%	11	7	12	10	12	8

[1] Values more than 100% indicate new normals higher than old ones.
[2] In cases with a limited difference between new and old climate normals, the frequencies of each tercile category would be 33% (i.e., 10 events over the 30-year period).

(HIRAI Masayuki, Tokyo Climate Center)

3. Climatological Normals for Monitoring of Global Warming

JMA monitors the long-term change of global average surface temperature (i.e., the combined average of near-surface air temperatures over land and sea surface temperatures) anomalies for the purpose of monitoring the global warming. Results are reported on the TCC website with monthly, seasonal and annual frequency, thereby helping to raise public awareness of climate change.

Following the introduction of JMA's new climatological normals in May 2021, the Agency replaced the 1981 – 2010 baseline period for global monitoring with that of 1991 – 2020, as well as land and ocean parts of combined data. The land part for the period before 2010 was updated from Version 2 to Version 4 of the Global Historical Climatology Network (GHCN) dataset provided by the U.S.A.'s National Climatic Data Center (NCDC), while data for the period since 2011 (CLIMAT messages archived at JMA) remains unchanged. The oceanic part, which consists of JMA's own long-term sea surface temperature analysis data, was updated from COBE-SST (Ishii et al. 2005) to COBE-SST2 (Hirahara et al. 2014).

Due to the new baseline period and the dataset update, the total global average percent coverage of JMA's new dataset is greater than before. The improvement in the coverage rate is particularly significant for the period after the 1990s because of an increased number of observation stations providing data for calculation.

JMA's new analysis indicates that the annual anomaly of the global average surface temperature for 2020, for example, was +0.34°C above the 1991 – 2020 average, and thus lower than the previous anomaly (+0.45°C above the 1981 – 2010 average). The reduced anomalies for each year mainly reflect the progress of global warming between the previous and new baseline periods (1981 – 2010 vs. 1991 – 2020). On a longer time scale, global average surface temperatures have risen at a rate of about 0.72°C per century, which is slightly lower than the previous analysis (0.75°C per century). These changes can be mainly attributed to the updates made to data and calculation methods.

In global average surface temperature analysis, anomalies for the period 1991 – 2020 from individual surface observations are calculated in relation to the 1991 – 2020 average. Conversely, those for the 20th-century average on the TCC website are first calculated in relation to the 1991 – 2020 average (the 1981 – 2010 average in the previous method) and then averaged over the globe before being adjusted to the 1901 – 2000 average.

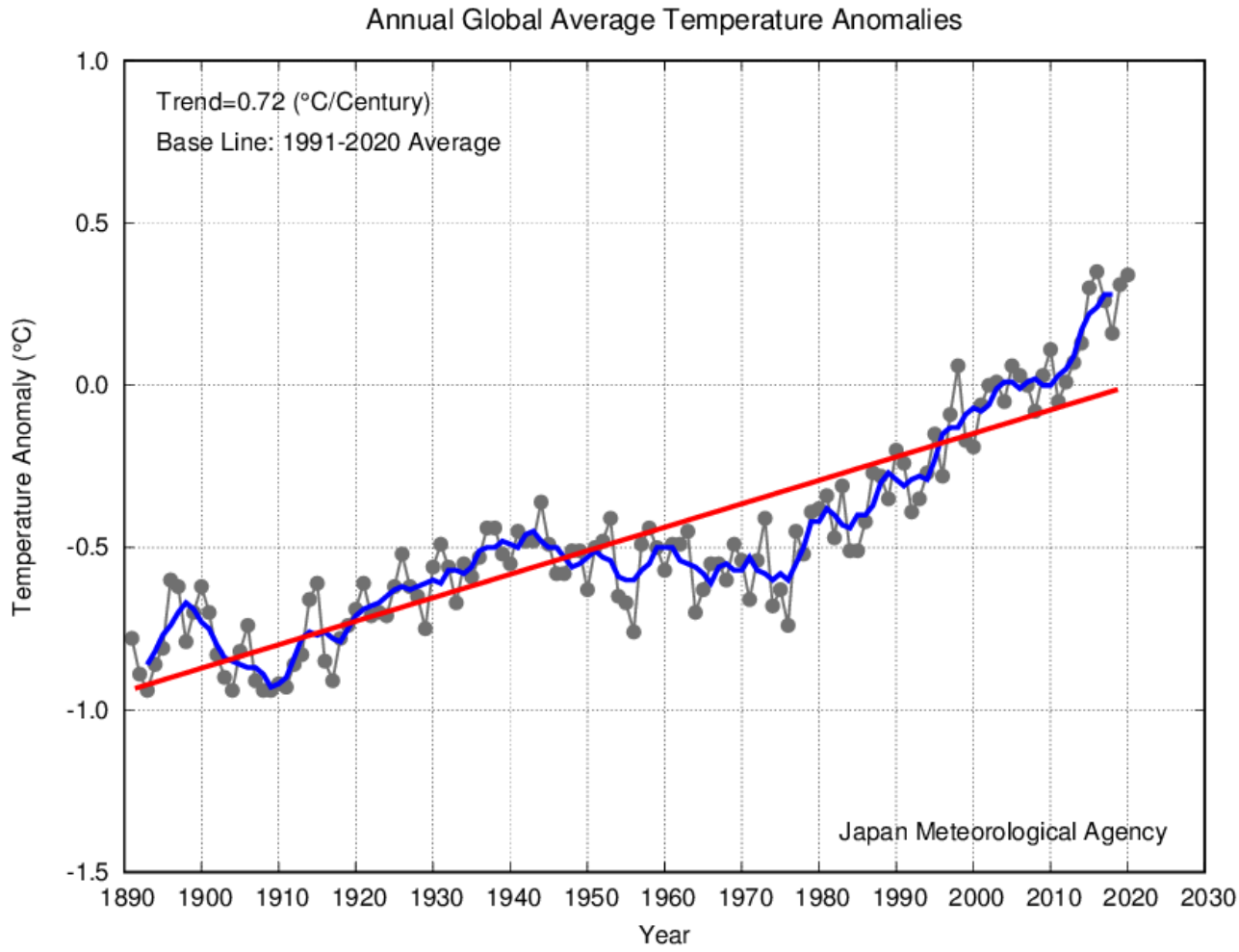

Figure 1-2 Annual anomalies of global average surface temperature

Anomalies are derived from the 1991 – 2020 average baseline. The thin black line indicates surface temperature anomalies for each year, while the blue and red lines indicate the related five-year running mean and the long-term linear trend, respectively.

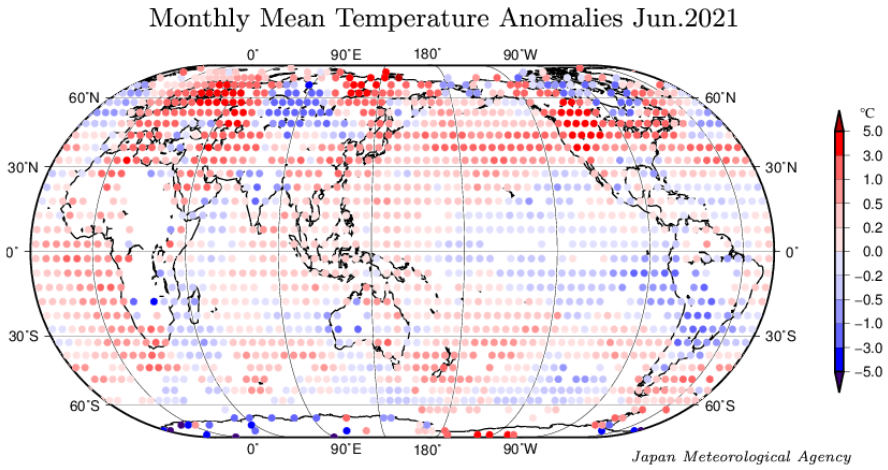

Figure 1-3 Distribution of surface temperature anomalies for June 2021

The circles indicate monthly anomalies of surface temperature averaged in 5° x 5° grid boxes. The monthly mean global temperature anomaly is determined by averaging the anomalies of all grid boxes weighted with the grid box area.

(TAMAKI Yuko, Tokyo Climate Center)

4. Worldwide Climatological Normals

JMA has started using new climatological normals based on the period from 1991 to 2020 to monitor the world climate.

As before, both data from CLIMAT Reports and those from the Global Historical Climatology Network monthly (GHCN-Monthly) dataset produced by the National Centers for Environmental Information of the National Oceanic and Atmospheric Administration (NOAA/NCEI) were used to produce the new normals. Version 4 (Menne et al. 2018) of the GHCN-Monthly dataset was used for temperature data, while Version 2 (Peterson and Vose 1997, Peterson et al. 1998) was used for precipitation data due to the absence of this information in Version 4.

The CLIMAT and GHCN-Monthly information was integrated into a single dataset for calculation of new normals for each observation station. Where both types of data were available for a particular station, CLIMAT (used for JMA's operational climate monitoring) was prioritized.

The GHCN-Monthly dataset and the integrated dataset were subjected to both automatic and manual quality control prior to calculation of the normals. Control protocols included testing to extract values that were unnaturally extreme, both in themselves and in comparison with surrounding stations (probably due to erroneous reading or reporting), and to detect artificial jumps in series of values and unnatural annual cycles (probably due to relocation of stations or changes in observation environments). As CLIMAT data are quality-controlled on an operational basis by JMA, no additional quality control was performed for calculation of the new normals.

Comparison between the New and Previous Normals

The new climatological normals were calculated for 5,189 surface temperature stations and 2,853 precipitation stations (except for Japanese stations) (Figure 1-4), as compared to the previous numbers of 2,549 and 2,658, respectively. The significantly increased number of stations from which data are now available in Southeast Asia supports enhanced climate monitoring.

The new normal temperatures are higher than the previous ones at most stations for every month (Figure 1-5 (a) and (b)). Unlike temperature, no homogeneous tendencies extending over the globe or for several consecutive months are observed between the new and previous normal precipitation amounts (Figure 1-5 (c) and (d)). However, some regional differences are seen. For instance, in January and December, the new normal precipitation amounts are higher for most stations on the Indochina Peninsula and around the South China Sea. In austral winter, values are lower for most stations in northeastern Australia.

(a) (b)

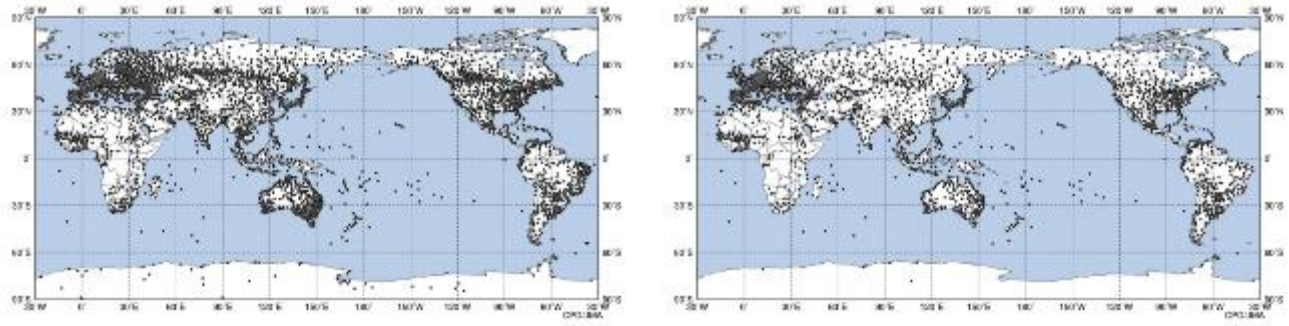

Figure 1-4 Distributions of climatological-normal stations for (a) surface temperature and (b) precipitation
Only stations with at least eight observations for every month from 1991 to 2020 are plotted on each map.

(a) (b)

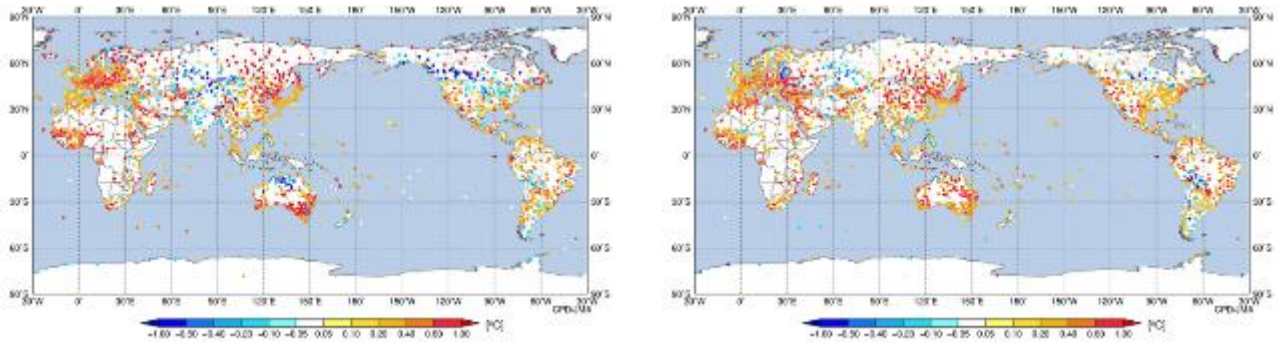

(c) (d)

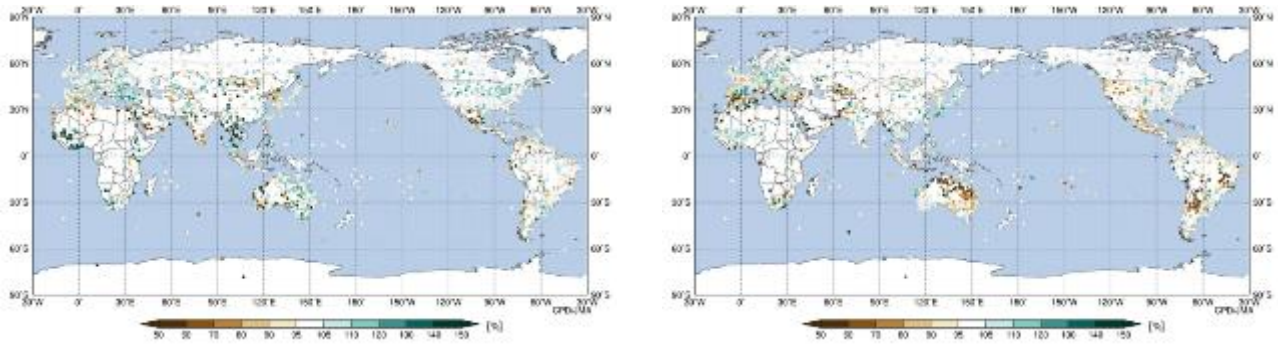

Figure 1-5 Differences between JMA's new and previous normal temperatures for (a) January and (b) July, and ratios of new to previous precipitation normals for (c) January and (d) July

(OKUNAKA Yuka and NISHIMURA Akio, Tokyo Climate Center)

5. Climatological Normals of Oceanographic Data

This section summarizes the characteristics of new climatological normals (1991 – 2020 average) in oceanographic data with comparison to the previous normals (1981 – 2010 average).

5.1 Sea Surface Temperatures

The new climatological normal of sea surface temperatures (SSTs) is based on COBE-SST (Ishii et al., 2005; Japan Meteorological Agency, 2006) as per the old ones. Figure 1-6 shows differences between the new and old normals for boreal summer (June – August) and winter (December – February). The new normals are higher than the previous ones in many parts of the world's oceans, particularly in the mid-latitude North Pacific and North Atlantic, and the Indian Ocean. This change is attributed to warm phases of decadal or multi-decadal variations in each ocean in the 2010s (the newly included decade in the baseline period for climatological normals) on top of the long-term warming trend (Figure 1-7). In the tropical Pacific, the difference between the new and old SST normals shows La Niña-like characteristics of warming in the western part and cooling or relatively weak warming in the eastern part over all seasons (not shown) , and particularly in boreal winter. The La Niña-like change in SST normals in the tropical Pacific is consistent with the long-term SST trend observed from 1891 to 2020 (Figure 1-7).

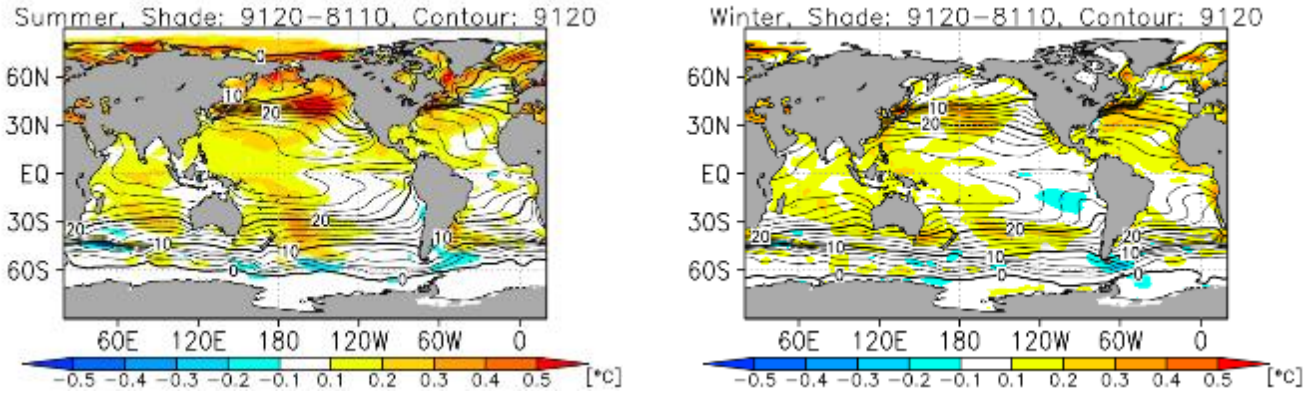

Figure 1-6 Differences between new and old SST normals

Shading shows differences between the new and old SST normals (1991 – 2020 and 1981 – 2010 averages, respectively) in °C for (a) boreal summer (June – August) and (b) winter (December – February). Contours indicate new SST normals at 2°C intervals.

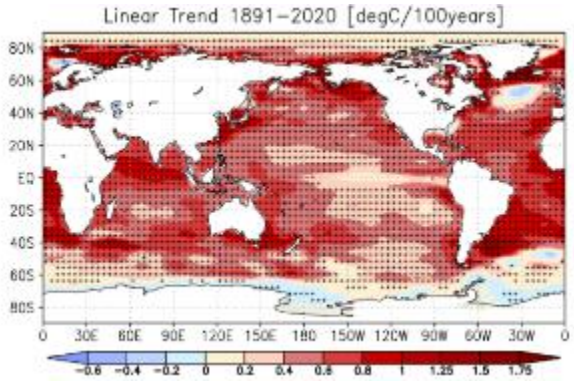

Figure 1-7 Linear trend of annual mean sea surface temperature from 1891 to 2020 (°C per century)

Plus signs indicate statistically significant trends with a confidence level of 95%.

5.2 Subsurface Water Temperatures

JMA also operationally analyzes ocean subsurface temperatures based on the ocean data assimilation system (MOVE/MRI.COM-G2, Toyoda et al., 2013) for monitoring of climate system phenomena including El Niño/La Niña and Indian Ocean Dipole events. Figure 1-8 shows differences between the new and old normals of ocean heat content (OHC) for boreal winter. These exhibit characteristics similar to typical OHC anomalies seen in La Niña events, corresponding to the SST changes in the tropical Pacific (Figure 1-6). The Pacific equatorial thermocline in the new normals is deeper than the previous one in the western part in association with a deep, warm subsurface layer, while a shallower thermocline is seen in the eastern part (Figure 1-9). Pacific trade winds in the new normal are generally stronger than in the old data (Section 6). These characteristics are consistent with those of differences between the new and old SST and OHC normals as described above.

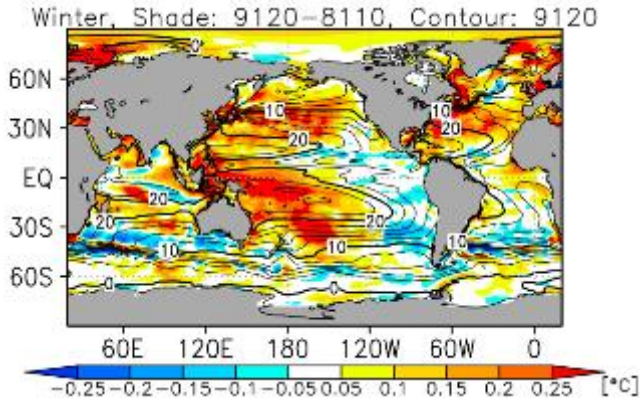

Figure 1-8 Differences between new and old OHC normals
Shading shows differences between the new and old OHC normals (1991 – 2020 and 1981 – 2010 averages, respectively) in °C for boreal winter (December – February). Contours indicate new OHC normals at 2°C intervals.

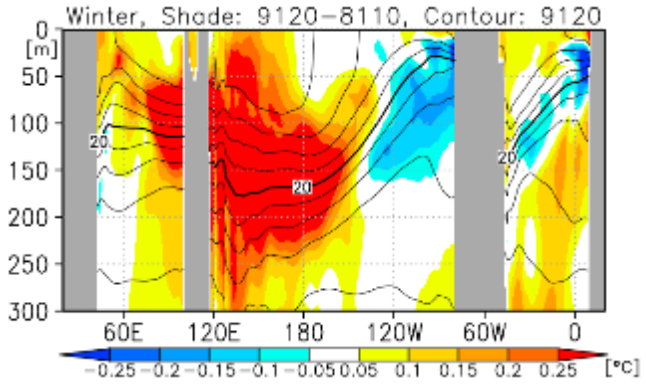

Figure 1-9 Depth-longitude cross section of temperatures along the equator
Shading shows differences between the new and old temperature normals (1991 – 2020 and 1981 – 2010 averages, respectively) in °C for boreal winter (December – February). Contours indicate new temperature normals at 2°C intervals.

(SATO Hirotaka and NISHIMURA Akio, Tokyo Climate Center)

6 Climatological Normals of Atmospheric Circulation Fields

This section briefly describes new normals of atmospheric circulation fields and summarizes related characteristics compared to the previous normals (i.e., the 1981 – 2010 average).

The data used for monitoring and analyzing atmospheric circulation are the Japanese 55-year Reanalysis (JRA-55; Kobayashi et al. 2015). The new atmospheric circulation normals are derived from the JRA-55 data for the period from 1991 to 2020.

Reflecting global warming, tropospheric temperatures for the new normals are generally higher than those for the previous ones, while stratospheric temperatures for the new normals are lower (Figure 1-10).

In the tropics, convective activity for the new normals tends to be enhanced from the eastern Indian Ocean to the western Pacific, where upper-tropospheric large-scale divergence is strengthened (Figure 1-11). This difference is

thought to be associated with changes in sea surface temperature (SST) normals, which exhibit characteristics similar to those of La Niña conditions in the tropical Pacific and warming in the Indian Ocean (Section 5). In boreal summer (June – August), large-scale divergence in the upper troposphere is shifted equatorward over the area from the Indian Ocean to the western Pacific.

Figure 1-12 shows differences between the new and previous normals for 850-hPa stream function fields in boreal summer. Lower-tropospheric cyclonic circulation is strengthened over the Arabian Sea and the monsoon trough is weakened over the area from the South China Sea to the Philippines. The westward extension of the North Pacific Subtropical High over the seas south of Japan in the new normals is stronger than that in the previous normals. Over the Pacific, subtropical highs are strengthened in both hemispheres throughout the year, which indicates strengthened trade winds over the equatorial Pacific and is consistent with differences between the new and previous normals in SSTs and ocean heat content (Section 5).

Figure 1-13 shows differences between the new and previous normals for sea level pressure and 850-hPa temperature fields in the Northern Hemisphere in boreal winter (December – February). The Siberian High is strengthened over northern Eurasia and the Aleutian Low is weakened in the new normals. The changes in normals observed over the North Pacific are consistent with a phase variation of the Pacific Decadal Oscillation. Lower tropospheric temperatures in the Northern Hemisphere exhibit a general increase, particularly over the area around the Barents Sea and the Kara Sea, while decreases are seen over parts of central Eurasia.

Differences between the new and previous normals are relatively small compared to the inter-annual variability of circulation fields in most elements and regions with certain exceptions, such as zonal-mean tropospheric temperatures (Figure 1-10) and upper-tropospheric geopotential height in the tropics. It should be noted that differences in upper-tropospheric large-scale convergence over Africa may have been affected by excessive convection biases over the area during the 1980s in JRA-55.

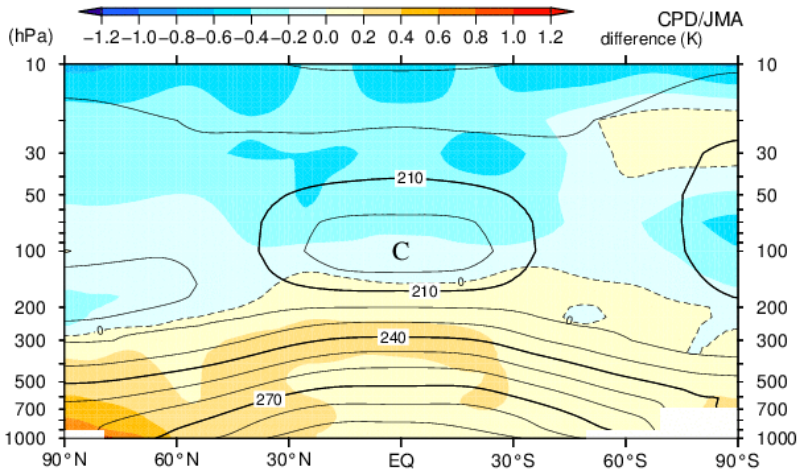

Figure 1-10 Latitude-height cross section of differences between new and previous normals for annual-mean zonal-mean temperature [K]
Shading indicates temperature deviations in the new normals from the previous normals. Contours show temperature for the new normals.

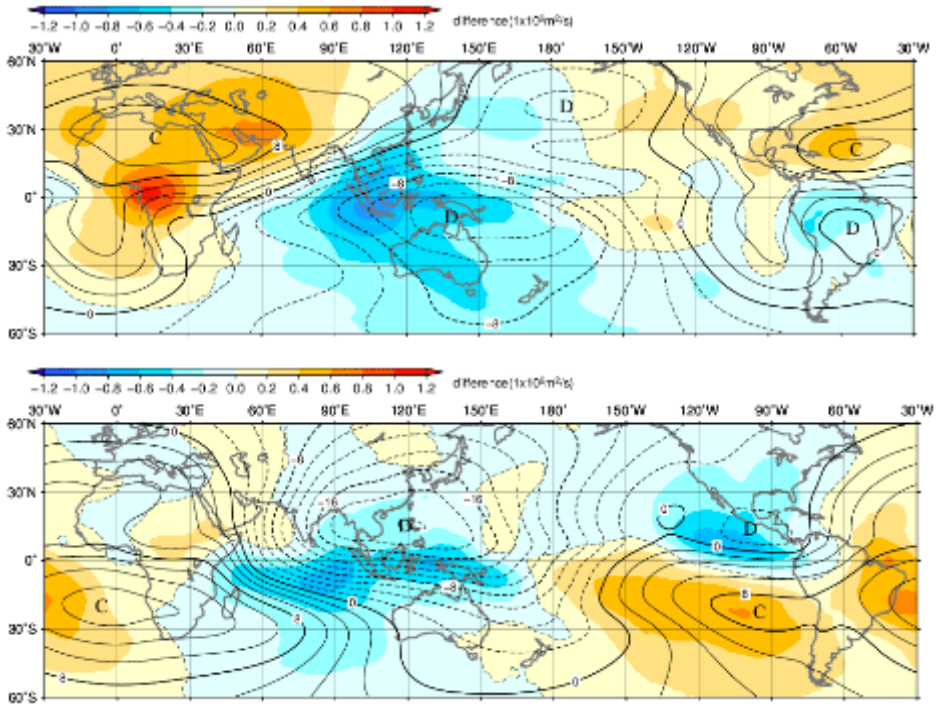

Figure 1-11 Differences between new and previous normals for 3-month mean 200-hPa velocity potential [$10^6 m^2/s$] (top: December – February; bottom: June – August)

Shading indicates velocity potential deviations in the new normals from the previous normals. Contours show velocity potential for the new normals.

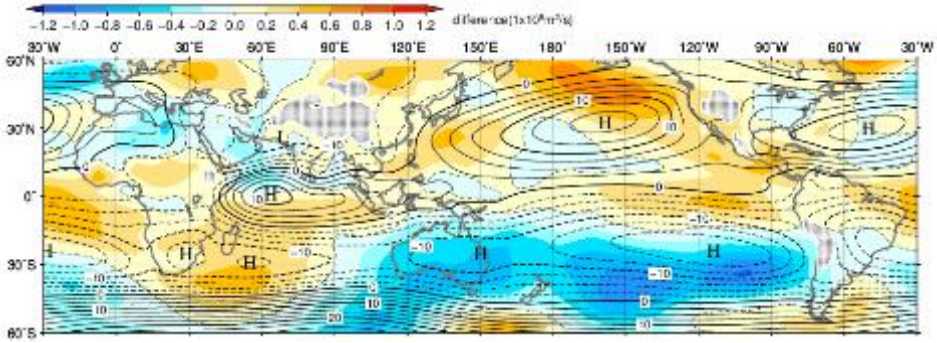

Figure 1-12 As per Figure 1-11, but for 850-hPa stream function [$10^6 m^2/s$] for June – August

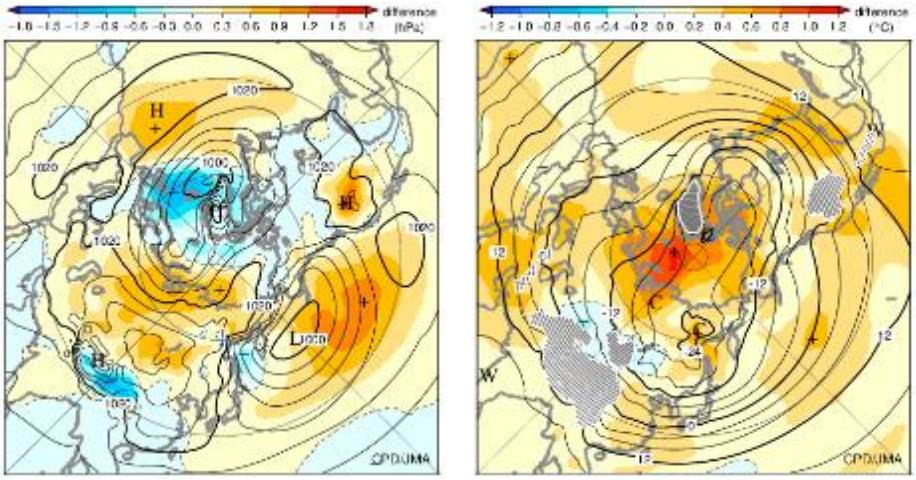

Figure 1-13 As per Figure 1-11, but for sea level pressure [hPa] (left) and 850-hPa temperature [°C] (right) for December – February

(SATO Hitoshi and SATO Hirotaka, Tokyo Climate Center)

References

Ishii, M., A. Shouji, S. Sugimoto, and T. Matsumoto, 2005: Objective Analyses of Sea-Surface Temperature and Marine Meteorological Variables for the 20th Century using ICOADS and the Kobe Collection. *Int. J. Climatol.*, **25**, 865 – 879.

Japan Meteorological Agency, 2006: Characteristics of Global Sea Surface Temperature Analysis Data (COBE-SST) for Climate Use. *Monthly Report on Climate System Separated Volume*, **12**, 116pp.

Kobayashi, S., Y. Ota, Y. Harada, A. Ebita, M. Moriya, H. Onoda, K. Onogi, H. Kamahori, C. Kobayashi, H. Endo, K. Miyaoka, and K. Takahashi, 2015: The JRA-55 Reanalysis: General specifications and basic characteristics. *J. Meteor. Soc. Japan*, **93**, 5 – 48.

Menne, M. J., C. N. Williams, B.E. Gleason, J. J Rennie, and J. H. Lawrimore, 2018: The Global Historical Climatology Network Monthly Temperature Dataset, Version 4. *J. Climate*, in press. doi: 10.1175/JCLI-D-18-0094.1

Peterson, T. C., and R. S. Vose, 1997: An overview of the Global Historical Climatology Network temperature database. *Bulletin of the American Meteorological Society*, **78**, 2837 – 2849

Peterson, T.C., R. Vose, R. Schmoyer, and V. Razuvaev, 1998: Global Historical Climatology Network (GHCN) quality control of monthly temperature data. *International Journal of Climatology*, **18**, 1169 – 1179

Toyoda T., Y. Fujii, T. Yasuda, N. Usui, T. Iwao, T. Kuragano, and M. Kamachi, 2013: Improved analysis of seasonal-interannual fields using a global ocean data assimilation system. *Theoretical and Applied Mechanics Japan*, **61**, 31 – 48.

<<Table of contents <Top of this article

JMA's Seasonal Ensemble Prediction System Upgrade Plan

The Japan Meteorological Agency (JMA) plans to upgrade its Seasonal Ensemble Prediction System (Seasonal EPS) from JMA/MRI-CPS2 to JMA/MRI-CPS3 (Table 2-1) in the first quarter of 2022. The seasonal EPS is based on a coupled atmosphere ocean model developed jointly by JMA and the Meteorological Research Institute (MRI).

The new seasonal EPS will have enhanced horizontal and vertical resolution for atmosphere and ocean considerations. The significant enhancement of horizontal resolution for atmosphere components will be double (TL319; approx. 55 km), and that for ocean components will be between double and quadruple (eddy-permitting resolution; 0.25 x 0.25 degrees). The initial atmospheric condition for operational forecasting will be changed from the Japanese 55-year Reanalysis (JRA-55) to global early analysis, as per the configuration for short-range to 1-month forecast systems, while that for the re-forecast (hindcast) system will be upgraded from JRA-55 to the new JRA-3Q reanalysis (the Japanese Reanalysis for Three Quarters of a Century; Table 2-2). Data assimilation for the oceanic initial condition in the operational and re-forecast (hindcast) systems will also be upgraded from 3DVAR to a combination of 4DVAR and Intermittent Analysis Update (IAU) with the new 3DVAR sea-ice initialization.

The ensemble size and running frequency of operational forecasting will be changed from 13 ensemble members every 5 days to 5 ensemble members every day, thereby enabling dispersion of computer resources and network traffic for acquisition and handling of gridded data as well as updating of seasonal forecasts on a daily basis. It should be noted that the baseline period for seasonal forecast products will also be changed to 1991 – 2020 along with implementation of the new seasonal EPS. 1.25-degree daily gridded data for six-month forecasts will be experimentally available on the TCC website from December 2021 onward.

Table 2-1 Comparison of the new seasonal EPS and the current seasonal EPS

Model	JMA/MRI-CPS3 (Next Model planned in the first quarter of 2022)	JMA/MRI-CPS2 (Current Model since June 2015)
Horizontal Resolution	- Atmosphere: TL319 (approx. 55km) - Ocean：0.25 ° (lon)×0.25 ° (lat)	- Atmosphere：TL159 (approx. 110km) - Ocean：1.0 ° (lon)×0.5-0.3 ° (lat)
Vertical Layers	- Atmosphere：100 levels (up to 0.01hPa) - Ocean：60 levels	- Atmosphere：60 levels (up to 0.1hPa) - Ocean：52 levels and Bottom Boundary Layer
Initial Condition for Forecast	- Atmosphere： Global Analysis - Land：Offline Land Analysis (*) - Ocean：4DVAR(coarse res) + IAU(eddy permitting res), daily (*) - Sea Ice：3DVAR, daily (*) * Forcing is given from Global Analysis	- Atmosphere：JRA-55 - Land：JRA-55 - Ocean：3DVAR at 5-day interval (*) - Sea Ice：Climatology * Forcing is given from JRA-55
Forecast Range	- 7 months (240 days)	- 7 months (240 days)
Number of Ensemble	- 5 members per an initial (51 members are used for JMA's statistical forecasts by a Lagged Average Forecast method)	- 13 members per an initial (51 members are used for JMA's statistical forecasts by a Lagged Average Forecast method)
Frequency of Forecast	- Every day	- Every 5 days
Re-forecast	- 24 initials x 5 members x 30 years (1991-2020)	- 24 initials x 5 members x 41years (1979-2019)
Initial Condition for Re-forecast	- Atmosphere：JRA-3Q - Ocean：4DVAR (JRA-3Q forcing)	- Atmosphere：JRA-55 - Ocean：3DVAR (JRA-55 forcing)

Table 2-2 Comparison of JRA-3Q and JRA-55

Reanalysis System	JRA-3Q (Next Re-analysis planned in Late 2021)	JRA-55 (Current Reanalysis since 2012)
Analysis Period	1947 - present	1958 - present
Data Assimilation System	Based on the operational analysis system as of December 2018.	Based on the operational analysis system as of December 2009.
Horizontal Resolution	TL479L100 (approx. 40 km)	TL319L60 (approx. 55 km)
Vertical Layers	100 levels (up to 0.01hPa)	60 levels (up to 0.1hPa)
Radiative transfer model for satellite radiance assimilation	RTTOV-10.2	RTTOV-9.3
SST and Sea-ice	COBE-SST2 before 1985 (1.0˚ x1.0˚) MGD-SST from 1985 onward (0.25˚ x0.25˚ using satellite data)	COBE-SST (1.0˚ x1.0˚)
Ozone	MRI-CCM2 (TL159L64)	Climate Value in and before 1978 MRI-CCM1 in and after 1979 (T42L68)

(YAMADA Takashi, World Meteorological Centre of Tokyo)

<<Table of contents <Top of this article

You can also find the latest newsletter from Japan International Cooperation Agency (JICA).

JICA's World (April 2021)

https://www.jica.go.jp/english/publications/j-world/2104.html

JICA's World is the quarterly magazine published by JICA. It introduces various cooperation projects and partners along with the featured theme. The latest issue features "South Asia: The Beat of 1.8 Billion People".

Any comments or inquiry on this newsletter and/or the TCC website would be much appreciated.
Please e-mail to tcc@met.kishou.go.jp.
(Editors: KAKIHARA Koichiro and WAKAMATSU Shunya)

Tokyo Climate Center, Japan Meteorological Agency
3-6-9 Toranomon, Minato City, Tokyo 105-8431, Japan

TCC Website:
https://ds.data.jma.go.jp/tcc/tcc/index.html

<<Table of contents